

FIGURE 3. Correlation between uptake of ^{11}C -methionine and FDG measured as standardized uptake values ($r = 0.788$, $p < 0.01$).

detecting recurrent tumors after treatment, however, was similar with both tracers. Both agents showed a limited diagnostic sensitivity for small (<1.5 cm) tumors.

ACKNOWLEDGMENTS

We thank the Cook and Dunn Foundations for their financial support and Linda Haway for administrative assistance.

REFERENCES

1. Glazer HS, Lee JKT, Levitt RG, et al. Radiation fibrosis: differentiation from recurrent tumor by MR imaging. *Radiology* 1985;156:721-726.
2. Strauss LG, Conti PS. The applications of PET in clinical oncology. *J Nucl Med* 1991;32:623-648.
3. Inoue T, Kim EE, Komaki R, et al. Detecting recurrent or residual lung cancer with FDG-PET. *J Nucl Med* 1995;36:788-793.
4. Miyazawa H, Arai T, Iio M, Hara T. PET imaging of non-small-cell lung carcinoma

- with carbon-11-methionine: relationship between radioactivity uptake and flow-cytometric parameters. *J Nucl Med* 1993;34:1886-1891.
5. Lindholm P, Leskinen-Kallio S, Minn H, et al. Comparison of fluorine-18-fluorodeoxyglucose and carbon-11-methionine in head and neck cancer. *J Nucl Med* 1993;34:1711-1716.
6. Leskinen-Kallio S, Ruotsalainen U, Nägren K, Teräs M, Joensuu H. Uptake of carbon-11-methionine and fluorodeoxyglucose in non-Hodgkin's lymphoma: a PET study. *J Nucl Med* 1991;32:1211-1218.
7. Hamacher K, Coenen HH, Stöcklin G. Efficient stereospecific synthesis of no-carrier-added 2- ^{18}F -fluoro-2-deoxy-D-glucose using aminopolyether supported nucleophilic substitution. *J Nucl Med* 1986;27:235-238.
8. Zasadny KR, Wahl RL. Standardized uptake values of normal tissues at PET with 2-[fluorine-18]-fluoro-2-deoxy-D-glucose: variations with body weight and a method for correction. *Radiology* 1993;189:847-850.
9. Wong WH, Uribe J, Hicks K, Hu G. An analog decoding BGO block detector using circular PMT. *IEEE Nucl Sci Trans* 1995;42:(1095).
10. Minn H, Clavo AC, Gréman R, Wahl RL. In vitro comparison of cell proliferation kinetics and uptake of tritiated fluorodeoxyglucose and L-methionine in squamous-cell carcinoma of the head and neck. *J Nucl Med* 1995;36:252-258.
11. Kubota R, Kubota K, Yamada S, et al. Methionine uptake by tumor tissue: a microautoradiographic comparison with FDG. *J Nucl Med* 1995;36:484-492.
12. Kubota R, Kubota K, Yamada S, Tada M, Ido T, Tamahashi N. Microautoradiographic study for the differentiation of intratumoral macrophages, granulation tissues and cancer cells by the dynamics of fluorine-18-fluorodeoxyglucose uptake. *J Nucl Med* 1994;35:104-112.
13. Griffith LK, Dehdashti F, McGuire AH, et al. PET evaluation of soft-tissue masses with fluorine-18-fluoro-2-deoxy-D-glucose. *Radiology* 1992;182:185-194.
14. Okazumi S, Isono K, Enomoto K, et al. Evaluation of liver tumors using fluorine-18-fluorodeoxyglucose PET: characterization of tumor and assessment of effect of treatment. *J Nucl Med* 1992;33:333-339.
15. Fujiwara T, Matsukawa T, Kubota K, et al. Relationship between histologic type of primary lung cancer and carbon-11-L-methionine uptake with positron emission tomography. *J Nucl Med* 1989;30:33-37.
16. Leskin-Kallio S, Nägren K, Lehtikainen P, Ruotsalainen U, Teräs M, Joensuu H. Carbon-11-methionine and PET is an effective method to image head and neck cancer. *J Nucl Med* 1992;33:691-695.
17. Kubota K, Ishiwata K, Kubota R, et al. Tracer feasibility for monitoring tumor radiotherapy: a quadruple tracer study with fluorine-18-fluorodeoxyglucose or fluorine-18-fluorodeoxyuridine, L-[methyl- ^{14}C]methionine, [6- ^3H]thymidine, and gallium-67. *J Nucl Med* 1991;32:2118-2123.
18. Slosmon DO, Pittet N, Donath A, Polla BS. Fluorodeoxyglucose cell incorporation as an index of cell proliferation: evaluation of accuracy in cell culture. *Eur J Nucl Med* 1993;20:1084-1088.
19. Lapela M, Leskinen-Kallio S, Varpula M, et al. Imaging of uterine carcinoma by carbon-11-methionine and PET. *J Nucl Med* 1994;35:1618-1623.
20. Langer K-J, Braun U, Kops ER, et al. The influence of plasma glucose levels on fluorine-18-fluorodeoxyglucose uptake in bronchial carcinomas. *J Nucl Med* 1993;34:355-359.

Comparison of Fluorine-18-FDG PET and Technetium-99m-MIBI SPECT in Evaluation of Musculoskeletal Sarcomas

Jose R. Garcia, E. Edmund Kim, Franklin C.L. Wong, Melina Korkmaz, Wai-Hoi Wong, David J. Yang and Donald A. Podoloff
Department of Nuclear Medicine, the University of Texas M. D. Anderson Cancer Center, Houston, Texas

We compared the diagnostic accuracy of ^{18}F FDG PET and $^{99\text{m}}\text{Tc}$ -MIBI SPECT in musculoskeletal sarcomas. **Methods:** Forty-eight patients with clinically suspected recurrent or residual musculoskeletal sarcomas were examined with both FDG-PET and MIBI-SPECT within 2 wk of each study (one follow-up study in nine patients and two follow-up studies in one patient). Imaging findings were visually inspected with grading scales in conjunction with CT and/or MRI, and count-density ratios of lesion-to-contralateral area and standard uptake values (SUVs) of FDG and MIBI in lesions were also generated. The results were correlated with histologic findings (in 51 studies) and/or long-term follow-up evaluations. **Results:** The diagnostic sensitivities and specificities were 98% and 90% using FDG, and 81.6% and 80% using MIBI, respectively, with statistical signif-

icance in the sensitivity. The tumors were demonstrated better in FDG studies, which produced higher visual grades (2.1 versus 1.6), and the tumors showed increasing SUVs with time (from 6.3 to 7.3). Four of nine patients with positive FDG but negative MIBI scans failed to respond to multidrug therapy. **Conclusion:** FDG-PET and MIBI-SPECT are useful in differentiating active sarcomas from post-treatment changes and in evaluating therapeutic response. MIBI-SPECT and FDG-PET findings should be interpreted in conjunction with CT and/or MRI. FDG-PET shows statistically significant higher sensitivity than MIBI-SPECT. A positive FDG but negative MIBI scan might suggest a multidrug resistance.

Key Words: sarcomas; fluorine-18-fluorodeoxyglucose; PET; technetium-99m-sestamibi; SPECT

J Nucl Med 1996; 37:1476-1479

Received Sept. 11, 1995; revision accepted Mar. 6, 1996.

For correspondence or reprints contact: E. Edmund Kim, MD, Department of Nuclear Medicine, The University of Texas M. D. Anderson Cancer Center, 1515 Holcombe Blvd., Box 59, Houston, TX 77030.

The diagnosis of residual or recurrent bone and soft-tissue masses remains a diagnostic dilemma in clinical practice. CT

TABLE 1
Number of Musculoskeletal Sarcomas in Various
Histological Types

Osteogenic sarcoma	18 (4 twice)
Malignant fibrous histiocytoma (MFH)	7 (2 twice)
Ewing's sarcoma	5
Chondrosarcoma	5
Synovial sarcoma	4 (2 twice)
Alveolar sarcoma	3 (1 three times)
Leiomyosarcoma	3 (1 twice)
Neurofibrosarcoma	1
Ganglioneuroblastoma	1
Myxoid sarcoma	1

The numbers in parentheses indicate the patients who underwent more than one study, and the follow-up studies were performed within 4–11 mo after the initial studies.

and MRI are excellent tools for visualizing anatomic detail, extent of disease and lesion characteristics. However, morphologic findings are not sufficiently reliable indicators of active tumor tissue, malignant or benign, especially during therapy. Tumor recurrence and post-treatment changes cannot be accurately differentiated by these conventional imaging techniques (1–3). In contrast, [¹⁸F]fluorodeoxyglucose (FDG) PET or ^{99m}Tc-hexakis(2-methoxyisobutylisonitrile) (MIBI) SPECT depict the metabolic derangements associated with abnormal tissues, providing critical information about the biological activity of musculoskeletal tumors that cannot be obtained with other modalities. The purpose of our study was to evaluate the potential of FDG-PET and MIBI-SPECT to distinguish viable tumor from fibrosis in areas of radiologic abnormalities after various treatments of musculoskeletal sarcomas and to compare the sensitivity and specificity of these two agents for the diagnosis of residual or recurrent musculoskeletal sarcoma.

MATERIALS AND METHODS

Patients

The study group included 48 patients (24 women, aged 17–68 yr, mean age 41 yr, 24 men, aged 16–65 yr, mean age 39 yr) with a variety of bone and soft-tissue sarcomas who have undergone various treatments (surgery, chemotherapy, and radiotherapy). Because of suspicion of recurrent or residual sarcomas based on clinical and/or imaging findings after 1 mo to 8 yr after the last therapy, FDG-PET and MIBI-SPECT were performed once in all patients, twice in nine patients and three times in one patient. Fifty-nine combined studies were analyzed in all. Lesion size ranged from 1.5 to 9.5 cm. The types of sarcoma encountered and the number of incidences of each type are listed in Table 1. The anatomic locations of these lesions are listed in Table 2.

In the 39 patients, the final diagnosis was established with positive PET and SPECT studies as well as in 12 patients with

TABLE 2
Anatomic Locations of Lesions

Head and neck	3 (2 twice)
Thorax	10 (2 twice)
Abdomen	3 (1 twice)
Pelvis	13 (2 twice)
Upper extremity	6 (1 twice)
Lower extremity	13 (1 three times, 1 twice)

Numbers in parentheses are the patients who underwent more than one study.

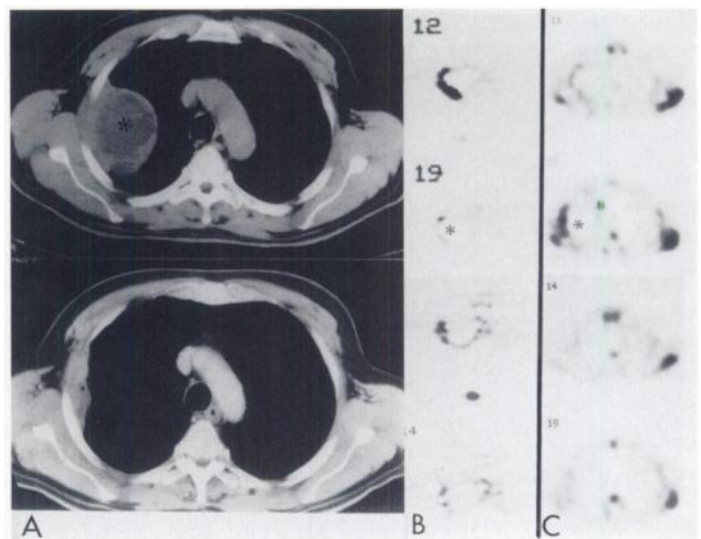


FIGURE 1. MFH of right chest wall (true-positive scan). Axial images of CT (A) and FDG-PET (B) show marked improvement of the mass lesion with central necrosis (*) and significant reduction of FDG uptake on follow-up studies (bottom). There is no abnormally increased MIBI uptake on follow-up MIBI-SPECT (C, bottom). Residual tumor was found at surgery.

discordant studies (positive with one tracer and negative with the other) by histologic examinations within 1 mo after the imaging studies. The results for the eight patients with negative FDG and MIBI studies were confirmed by clinical follow-up for at least 6 mo after the two tests.

Imaging

The FDG-PET and MIBI-SPECT studies were obtained in less than 15 days in all patients. FDG-PET studies were performed using a scanner that provides a 42-cm vertical and 11-cm axial field of view. Sensitivity is approximately 120,000 cps/ μ Ci/ml, and the reconstructed tranaxial resolution is about 5.8 mm FWHM. After obtaining an attenuation scan using a ⁶⁸Ge/⁶⁷Ga rotating sector source, 10 mCi [¹⁸F]FDG were administered intravenously after at least 4 hr of fasting. Three consecutive sets of transaxial images were taken (at 1–20 min, 21–40 min and 41–60 min, respectively), and coronal and/or sagittal reconstructed images were also obtained. The count-density ratios of the lesion-to-contralateral area were calculated by placing regions of interest over the peak activity in the lesion and normal contralateral area. Semiquantitative evaluation, using standard uptake value (SUV) color-coded images, was made in addition to visual inspection of the images. SUV were obtained as follows:

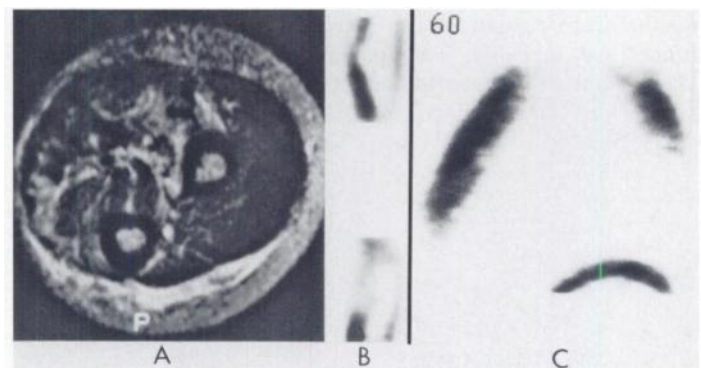


FIGURE 2. MFH of left forearm (false-positive scan). T2-weighted axial image of left forearm (A) shows heterogeneously increased signal intensity in flexor muscle and subcutaneous lymphedema in medial-posterior aspect. Sagittal FDG-PET image (B) shows diffusely increased activity in the volar aspect of left forearm. Coronal MIBI-SPECT image (C) shows diffusely increased activity in the left forearm.

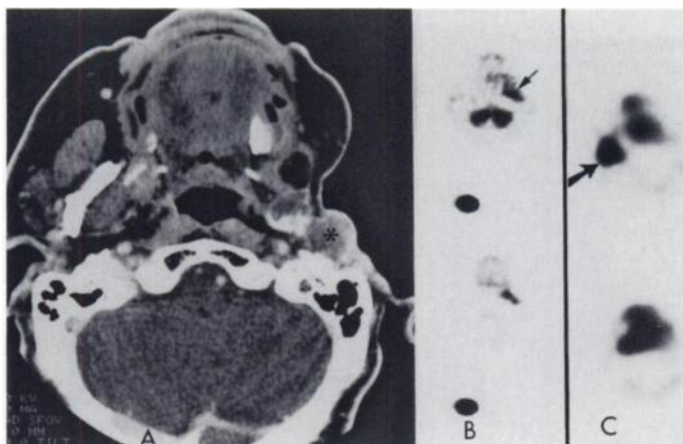


FIGURE 3. Osteosarcoma of left ear canal (true-positive FDG and false-negative MIBI). Axial CT image of skull base (A) shows a nodular mass (*) in the left ear canal. Axial FDG-PET images of lower head (B) show markedly increased activity in the area of left ear canal (arrow), indicating metabolically active recurrent tumor, which was confirmed surgically. Axial MIBI-SPECT images (C) at comparable levels show no abnormally increased activity in the area of left ear canal. Note markedly increased activity (arrow) in the right parotid gland.

$$\text{SUV} = \frac{\text{Tissue concentration (mCi/g)}}{\text{Injected dose (mCi)/body weight (g)}}$$

Whole-body imaging was performed at 30–60 min after intravenous injection of 15 mCi ^{99m}Tc -MIBI using a dual-detector gamma camera with an ultra high-resolution collimator. SPECT images of abnormal areas were also obtained at 90–180 min after injection, using a triple-detector gamma-camera with an ultra high-resolution collimator (64 × 64, 40 sec/stop, 40 stop). The MIBI and FDG images were visually interpreted and carefully correlated with contemporaneous CT and/or MRI studies. Simple qualitative analysis of all images was performed by two nuclear medicine physicians, and consensus was then reached for final diagnosis of active tumor or post-treatment changes. The diagnostic sensitivity and specificity with ^{18}F FDG and ^{99m}Tc -MIBI were obtained and compared using Fisher's exact test. We graded uptakes of both tracers by visual inspection according to the following scale: 0 = negative, 1 = mild, 2 = moderate and 3 = marked. Visual scales with FDG and MIBI were compared using Student's t-test.

RESULTS

For the 39 patients with true-positive results (Fig. 1) and the 8 with true-negative results, the FDG-PET and MIBI-SPECT images were in agreement. The true-positive and true-negative results were related to the presence and absence of active tumors, respectively. Two patients had false-negative MIBI studies, one of whom also had a false-positive FDG study (Fig.

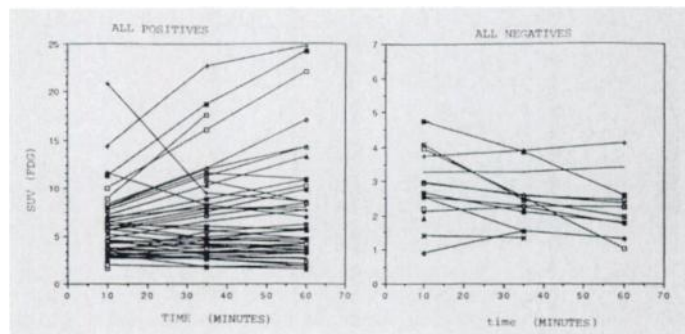


FIGURE 4. FDG SUV time-activity curves for patients with positive and negative studies.

2). Patients with false-positive scans also had inflammatory changes determined histologically. Nine patients had false-negative MIBI scans but true-positive FDG scans (Fig. 3). Follow-up studies in these patients showed a better reflection of histological and clinical results with changes in FDG uptake. Four patients had persistent true-positive FDG scans, but their MIBI scans were false-negative. These patients had fulminant courses with resistance to therapy. There was a significantly higher sensitivity with FDG than with MIBI (98% versus 81.6%; $p = 0.015$). The specificities with FDG and MIBI were 90% and 80%, respectively ($p = 1.000$). Positive and negative predictive values with FDG were 98% and 90%, respectively. Positive and negative predictive values with MIBI were 95.2% and 87.1%, respectively. There was a statistically significant difference (using the Student's t-test) between the results of the visual analysis for the patients undergoing MIBI and FDG imaging, with a better detection of active sarcoma with FDG. The visual scales with FDG and MIBI were 2.103 ± 1.150 and 1.655 ± 1.332 , respectively ($p = 0.0006$). The mean lesion-to-contralateral count-density ratios were 2.57 ± 1.29 for sarcoma lesions and 1.29 ± 0.37 for post-treatment changes. The average SUV in serial images of all patients with positive PET scans shows increasing FDG uptake in active tumors over time (average SUV = 6.32, 7.05, and 7.30 on 20, 40, and 60 min, respectively). The FDG SUV time-activity curves for patients with the positive and negative scans shown in Figure 4. Visual analysis of color-coded SUV FDG images is more accurate in minimizing false-positives than in the visual inspection of nonquantitative FDG images.

DISCUSSION

The development of radical surgical techniques combined with chemotherapy, radiotherapy and reconstructive surgery resulted in the need for accurate postoperative follow-up studies. Despite advances in CT and MRI, current technology remains unsatisfactory, particularly in differentiating viable tumor from necrosis after treatment because of changes in normal anatomy and the distortion of normal tissue planes (1–3). Various radiopharmaceuticals have been proposed as bone and soft-tissue tumor imaging agents. The use of ^{67}Ga -citrate, which has poor physical characteristics, has been limited because it necessitates long waiting periods after injection and because of its lack of specificity. Although ^{99m}Tc -methylenediphosphonate (MDP) can localize primary and metastatic sites of tumors in the skeletal system, it is a nonspecific agent that also demonstrates the healing process. Thallium-201-chloride has been proposed for detection of active bone and soft-tissue tumors, yet its long biological half-life limits the administered dose, frequently resulting in long imaging times and poor image quality (4,5).

MIBI belongs to a class of lipophilic cationic agents that were introduced as myocardial perfusion imaging agents in the 1970s and approved by the FDA in the 1990s. Technetium-99m-MIBI has biological properties similar to ^{201}Tl , which has proved to be of value in evaluating tumor activity. Despite the higher photon flux of ^{99m}Tc -MIBI, there was no statistically significant difference between these two agents (6–8). The mechanism of MIBI uptake in the tumors is uncertain, but it appears to be related to mitochondrial activity and plasma membrane potential. Technetium-99m-MIBI is also delivered by normal blood flow, so the vascular supply to the tumor site must be intact (9). Regardless of the radionuclide uptake mechanism, MIBI has been useful in the detection of musculoskeletal sarcomas (10,11). FDG as an indicator of regional glucose metabolic rate has been effective in clinical oncology.

Tumor imaging with FDG is based on the hypothesis that the rate of anaerobic glycolysis increases with differentiation of tumor cells and with an increasing grade of malignancy (12). Several different neoplasms have been imaged with FDG since the first demonstration of its ability to localize cerebral gliomas (13). FDG-PET has shown potential in helping to distinguish malignant lesions from metabolically inactive tissue and in providing unique information about the distribution of active tumor relative to necrotic or nonmalignant tissue stroma or to inflammatory or postoperative change (14). Malignant tissues (dedifferentiation of tumor cells and an increased grade of malignancy) have an increased rate of anaerobic glycolysis. FDG is transported into tissues and cells by the same carrier-mediated mechanisms responsible for the transport of glucose. Once in the cell, FDG is rapidly phosphorylated by intracellular hexokinase. As a deoxyglucose analog, FDG competes with natural glucose for transport and phosphorylation. Once in the cell, it is transformed into fluorodeoxyglucose-6-phosphate and becomes trapped without further metabolism. Visual analysis of PET images as well as semiquantitative evaluation using SUVs of FDG accumulation with contemporaneous CT or MRI studies may offer unique information about the nature of tumor lesions. This metabolic information may prove valuable in many patients and may influence decisions on intervention versus close clinical observation of lesions. It also can guide the surgeon to the most metabolically active tissue sites for biopsy, especially in lesions in which there is regional heterogeneity.

PET imaging of musculoskeletal masses does have certain pitfalls given its limited resolution (8,15). There must also be some concern about the natural variability of FDG accumulation in benign or malignant processes, since numerous factors (i.e., blood flow, plasma glucose concentration and tissue hexokinase activities) in addition to glucose metabolic rate determine FDG accumulation.

In our study, the use of SUVs differentiated active sarcomas (>3 SUV) from post-treatment changes (<3 SUV). As whole-body imaging becomes more readily available, it will be possible to search for missed lesions or distant metastases as well. Our study also demonstrates that the treatment significantly inhibits MIBI uptake and thus may be used to evaluate the effectiveness of therapy. In nine patients, MIBI studies were false-negative despite the presence of active sarcoma histologically. Follow-up studies in these patients continued to result in true-positive FDG scans, but four patients also had false-negative MIBI studies. These patients had fulminant courses that were resistant to therapy. The multidrug-resistant P-glycoprotein (Pgp) encoded by the mammalian multidrug resistance gene (MDR1) appears to function as an energy-dependent efflux pump. Many drugs interacting with Pgp are lipophilic and cationic at physiologic pH.

Piwnica-Worms et al. (16) have demonstrated enhanced extrusion of ^{99m}Tc-sestamibi by Pgp-enriched cells as well as enhanced uptake of ^{99m}Tc-sestamibi by multidrug-resistant reversal agents such as verapamil and cyclosporin A in a nude mouse tumor model. Their results indicate that ^{99m}Tc-sestamibi is a transport substrate recognized by Pgp and ultimately provides a means to direct patients to specific cancer therapies. Although our four patients with negative MIBI but positive FDG scans were drug-resistant, more patient studies are needed to differentiate drug resistance from decreased membrane

permeability of active tumor cells since our five other patients with decreasing MIBI uptake demonstrated good responses to chemotherapy. Lastly, it appears relatively difficult to evaluate MIBI and FDG uptake in tumors located near the heart, kidney and bladder since normal activities in the gastrointestinal and urinary tracts might obscure underlying abnormalities, especially with MIBI. Normal MIBI uptake in skeletal muscle, salivary gland, nasopharyngeal mucosa, pituitary gland and choroidal plexus could potentially limit the detection of tumors in these organs. These difficulties are partially solved with the use of three-dimensional display and serial imaging and through correlation with morphologic studies such as CT and MRI.

CONCLUSION

FDG-PET and MIBI-SPECT are useful adjunct tools in the evaluation of musculoskeletal sarcomas, particularly in distinguishing between benign and malignant tissue components and in distinguishing sarcoma from post-therapeutic changes. FDG-PET appears to be more sensitive in detecting active musculoskeletal sarcomas than MIBI-SPECT. However, negative MIBI but positive FDG scans might suggest a multidrug-resistant condition. We propose a strategy in which these techniques are used to monitor patients who are undergoing cancer treatment. If there is clinical or histological evidence of recurrence but the MIBI-SPECT is negative, a more expensive FDG-PET scan is recommended to investigate possible drug-resistance or, in case of a positive FDG scan, biopsy for active sarcoma.

REFERENCES

1. Aisen AM, Martel W, Braunstein EM, Phillips WA, Kling TF. MRI and CT evaluation of primary bone and soft-tissue tumors. *AJR* 1986;146:749-756.
2. Hudson TM, Hamlin DJ, Enneking WF, Pettersson H. Magnetic resonance imaging of bone and soft-tissue tumors: early experience in 31 patients compared with computed tomography. *Skeletal Radiol* 1985;13:134-146.
3. Petasnick JP, Turner DA, Charters JR, Gitelis S, Zacharias CE. Soft-tissue masses of the locomotor system: comparison of MR imaging with CT. *Radiology* 1986;160:125-133.
4. Ramanna L, Waxman A, Binney G, Mirra J, Rosen G. Thallium-201 scintigraphy in bone sarcoma: comparison with gallium-67 and technetium-99m-MDP in the evaluation of chemotherapeutic response. *J Nucl Med* 1990;31:567-572.
5. Podoloff DA, Haynie TP, Kim EE, et al. Thallium-201 SPECT tumor imaging in differentiation of recurrent metastases disease from post-therapy complications. *J Nucl Med* 1993;32[Abstract]:962.
6. O'Tuama L, Treves S, Larar J, et al. Thallium-201 versus technetium-99m-MIBI SPECT in evaluation of childhood brain tumors: within-subject comparison. *J Nucl Med* 1991;34:1045-1051.
7. O'Tuama L, Packard A, Treves S. SPECT imaging of pediatric brain tumor with hexakis (methoxyisobutylisocyanide) technetium (I). *J Nucl Med* 1990;31:2040-2041.
8. Adler L, Blair H, Makley J, et al. Noninvasive grading of musculoskeletal tumors using PET. *J Nucl Med* 1991;32:1508-1512.
9. Hassan I, Sahweil A, Constantinides C, et al. Uptake and kinetics of ^{99m}Tc-hexakis 2-methoxy isobutyl isocyanide in benign and malignant lesions in the lungs. *Clin Nucl Med* 1989;14:333-340.
10. Caner B, Kitapci M, Unlü M, et al. Technetium-99m-MIBI uptake in benign and malignant bone lesions: comparative study with technetium-99m-MDP. *J Nucl Med* 1992;33:319-324.
11. Caner B, Kitapci M, Aras T, Erben G, Ugur D, Bekdik C. Increased accumulation of hexakis (2-methoxyisobutylisocyanide) technetium (I) in osteosarcoma and its metastatic lymph nodes. *J Nucl Med* 1991;32:1977-1978.
12. Warburg O. On the origin of cancer cells. *Science* 1956;123:309-314.
13. Janus T, Kim EE, Tilbury R, Brunner JM, Yung WAF. Use of [¹⁸F]fluorodeoxyglucose positron emission tomography in patients with primary malignant brain tumors. *Ann Neurol* 1993;33:540-548.
14. Strauss L, Clorius J, Schlag P, et al. Recurrence of colorectal tumors: PET evaluation. *Radiology* 1989;170:329-332.
15. Griffith L, Dehdashti F, McGuire A, et al. PET evaluation of soft-tissue masses with fluorine-18-fluoro-2-deoxy-D-glucose. *Radiology* 1992;182:185-194.
16. Piwnica-Worms D, Chiu ML, Budding M, Kronause JF, Kramer RA, Croop JM. Functional imaging of multidrug-resistant P-glycoprotein with an organotechnetium complex. *Cancer Res* 1993;53:977-984.